Examination of Error Propagation in Relationships between Leaf Area Index and Spectral Vegetation Indices from Landsat TM and ETM

R. Fernandes, H.P. White, S. Leblanc, G. Pavlic, H. McNairn
Canada Centre for Remote Sensing
Natural Resources Canada
(613) 947-1297
rfernand@ccrs.nrcan.gc.ca

J.M. Chen
Department of Geography
University of Toronto
(416) 978-7085
chenj@geog.utoronto.ca

R. Hall
Canadian Forest Service
Natural Resources Canada
(780) 435-7209
rhall@cfs.nrcan.gc.ca

Abstract

Abstract – Leaf Area Index (*L*) is one biophysical parameter that has been extensively examined for its potential of routine and even automated estimation from remotely sensed signals. Maps of *L* are today regularly produced in Canada using Landsat imagery in conjunction with ground truth, by determining a relationship between a satellite based vegetation index and field measurements of *L*. To examine this technique, sites were visited across Canada during the 1998 and 2000 growing seasons. Common measurement standards were followed using the TRAC and LAI-2000 instruments, and some destructive shoot sampling was performed. In this paper, a semi-empirical method of scaling from ground based measures of *L* to 30 m resolution Landsat imagery using the Simple Ratio (*SR*) is documented and compared to purely empirical and purely model based approaches. Recent investigations into effects such as foliage clumping and canopy gap distributions allow for a more intensive error estimation of ground based *L* observations. Errors in producing at-surface reflectance and their propagation to the *L* -VI relationship were also examined for the *SR*.

Introduction

Leaf area index (*L*) is defined as half the total surface area of foliage per unit ground area projected on the horizontal datum (Fernandes et al., 2000). This definition stems from Levy and Madden (1933) who defined foliage area ratio as the area of foliage expressed as a percentage of ground area modified by Chen and Black (1992) by adding the term "half" to consider the various forms of leaves. allow some consistency in using *L* for canopy radiation estimation. However, it differs from all previous definitions we know of in that it is per unit horizontal projected ground area rather than per unit ground area (as defined in Chen and Black, 1992) to make it invariant to local slope. *L* is a quantitative measure of vegetation cover and an input to models of vegetation/atmosphere interactions including carbon, water and energy cycles. *L* can be estimated from measurements following (Nilson, 1971; Chen, 1996 and Kucharik et al., 2000):

$$L = \frac{\gamma_E(\theta)[1-\alpha(\theta)]\ln[P(\theta)]\cos\theta}{G(\theta)\Omega_E(\theta)\cos\beta} \quad (1)$$

Where P is the sub-canopy gap fraction, G is the fraction of foliage and Ω_E is the element clumping index, γ_E is the needle-to-shoot area ratio and $(1-\alpha)$ is the ratio of green to total plant area, all with respect to view angle θ relative to the local surface normal and β is the relative angle between the local surface normal and the horizontal datum.

In this study we use the *SR* to map *L*:

$$SR = \frac{\rho_{NIR}}{\rho_{RED}} \quad (2)$$

where ρ is the top-of-canopy hemispherical directional reflectance in red and near-infrared (NIR) wavelengths.

In general L and SR are both measured with error. Denote the set of available co-located (in time and space) measurements $C=\{(L',SR')\}$ as the calibration set. Estimation of L then corresponds to the estimating the marginal probability density function $p(L|SR')$. Empirical estimation methods use only C (e.g. Chen et al., 2001) while physical methods make no use of C (e.g. Knyazhikin et al., 1998). The goal of our study was to document and assess a semi-empirical approach to large area L estimation that was based on broadband spectral vegetation indices from moderate (30m) resolution Landsat imagery together with co-registered surface L measurements. In doing so we addressed the following questions:

1. What is the error in estimation of L from surface measurements and SR from Landsat?
2. What is the appropriate empirical regression predictions of $p(L|SR')$ for general land cover classes using Canada wide data sets?
3. How do empirical predictions with limited data compare to physical reflectance models?
4. Can we use a combination of empirical relationships and reflectance models to model uncertainty in L retrievals?

Study Sites and Data

Surface L measurements were conducted at 93 needleleaf, 113 broadleaf (including 18 agriculture) and 22 mixed sites across Canada during the 1998 and 2000 growing season. We omitted from consideration sites that deviated from green foliage, including certain agricultural sites, grasslands with substantial thatch, or forest canopies expressing hystological or stress related differences in leaf level reflectances. This was a limitation of our study necessitated by the reliance on a broadband SR.

P was measured using either the LAI-2000 and TRAC instruments as described in Chen et al. (1997). Sites were stratified across 9 World Reference System 2 Frames and within site transects were used to allow co-location of a 3x3 Landsat pixel block (Chen et al., 2001). Canopy clumping was measured using the TRAC over a subset of sites. Sites without Ω_E measurements were assigned the mean Ω_E for all sites of the same species. Both $\gamma$and α were estimated by destructive sampling as reported inby Chen et al. (1997) and Gower et al. (1999). Species mean values for $\gamma$and α were applied to all sites.

SR was derived from reflectance estimates from 8 Landsat 5 (TM5) Systematic Corrected nearest neighbour resampled data processed using (GICS , Radarsat International Inc.) and a L1G Landsat ETM scene processed using Landsat Processing Ground Segment (LPGS, United States Geological Survey). ETM radiances were back calibrated to equivalent radiances of the TM5 scenes using cross-calibration coefficients (Teillet et al. in press). Surface reflectance was estimated using 6S (Vermote et al., 1997) together with estimates of aerosol optical depth, water vapour and ozone concentrations (Chen et al., 2001) for the TM5 scenes and measurements of aerosol optical depth and water vapour from the AEROCAN network for the ETM scene.

Error Analysis of Surface L Measurements

Surface measurements of L were conducted such that the overstory foliage, defined as foliage for stems extending above 1.37m, was within the sensor field of view. This section provides an error analysis for estimation of overstory L assuming no contamination from understory foliage. Assuming measurement errors for terms in Equation 1 are uncorrelated, Gaussian and multiplicative the 1 standard deviation (1σ) relative error in L measurements is given by:

$$\varepsilon_L = \left[\varepsilon_{1-\alpha}^{\,2} + \varepsilon_{\gamma_E}^{\,2} + \varepsilon_{\ln P}^{\,2} + \varepsilon_G^{\,2} + \varepsilon_{\Omega_E}^{\,2}\right]^{0.5} \quad (3)$$

Where ε is the 1σ uncertainty in each subscripted parameter and we assume $\varepsilon_\theta=0$.

Chen (1996) cited ε_α from 5% to 12% for destructive sampling within a site. There is additional uncertainty when applying these estimates to other sites due to spatial variability and between species differences. Based on Gower et al. (1997) the coefficient of variation of stand mean stem area (S) is on the order of 50% for the jack pine stands to 25% for the aspen and black spruce. We use a 1σ value of 25% and assume it applies to total woody area (W). Whittaker and Woodwell (1967) report a relative difference in S between 31% to 40% when comparing of parabolic versus conic bole shapes. Assuming a symmetric distribution of differences ranging +/- 2σ gives a standard error estimate ranging from 7.5% to 10% due to stem shape uncertainty. Assuming the three error components are uncorrelated Gaussian and a S:W ratio of 0.5 (Gower et al., 1997) gives an ε_α of

27%. For a typical α of 0.2, $\varepsilon_{1-\alpha}$ is approximately 6%.

We assume $\gamma_E = 1$ and $\varepsilon_\gamma = 0$ for broadleaf stands. Measurement errors for γ_E in conifers is likely far less than the 7% to 20% observed range in γ_E between stands of the same species (Gower et al. 1999). To convert the observed range into a standard error we assume a mean value of γ_E is used and the range corresponds to +/-2σ. We therefore adopted a value of 3.5% for ε_γ conifers and 0 for deciduous.

Errors in TRAC estimates of Ω_E are reportedly less than 3.5% (Chen and Cihlar, 1995). However, a species mean Ω_E is applied to stands where the LAI-2000 is used to estimate P. The coefficient of variation of our measurements ranged from 5% for sugar maple to 14% for black spruce stands. We used a value of 6% for ε_Ω for broadleaf stands and 15% for conifer stands.

For θ between 30° and 60° G ranges from approximately 0.4 to 0.6 (Warren-Wilson, 1958). We used a value of 0.5 for all stands giving a mean ε_G of 7% assuming a uniform distribution of θ between 30° and 60° degrees

Under clear sky conditions and for θ less than 60° degrees the error in ln$P$ estimates from TRAC are less than 1%. Based on Leblanc and Chen (2001) 4th ring LAI-2000 estimates of ln$P$ are typically within 5% of ln$P$. However, the LAI-2000 estimates of ln$P$ in our database correspond to a weighted average for 5 annular rings based on Miller's Theorem (Miller 1963):

$$L = 2\int_0^{\pi/2} -\ln P(\theta)\sin\theta\cos\theta d\theta \qquad (4)$$

Formally, from Equation (1) Miller's Theorem requires modification (see Appendix A):

$$L = 2\int_0^{\pi/2} -\frac{\ln P(\theta)}{\Omega(\theta)}\sin\theta\cos\theta d\theta \qquad (5)$$

Furthermore, the LAI-2000 software uses a trapezoidal approximation to Equation 4 that may be sub-optimal. The possible bias errors for these factors may explain the consistent bias between L estimates using 4 versus a single ring or the TRAC and Equation 1 reported in Leblanc and Chen (2001). Leblanc and Chen (2001) also report that ln$P$ can be calibrated to within 2% of the fourth ring ln$P$ suggesting a total $\varepsilon_{\ln P}$ of 7%.

The total 1σ error budget for LAI estimates is less than 20% for conifer and 14% for broadleaf stands. The estimate for broadleaf stands is similar to the range of 11.5% to 13.5% reported in Oltoff et al. (2001).There is an additional error on the order of 0.25 LAI units due to unmeasured understory leaf area.

Error Analysis for Landsat SR

An analytical error analysis of SR is complicated by correlations in errors between component reflectances. We group errors into mutually uncorrelated components:

$$\varepsilon_{SR} = \left(\varepsilon_{atm}^2 + \varepsilon_{NIR/RED}^2 + \varepsilon_{red}^2 + \varepsilon_{NIR}^2\right)^{0.5} \qquad (6)$$

where ε_{atm} is the error in estimating the SR due to atmospheric correction of input radiances, $\varepsilon_{NIR/red}$ is the error in relative calibration or ρ_{NIR} and ρ_{red} (2% based on pre-launch calibration but assumed to have increased to 4%) and ε_{red} and ε_{NIR} are errors due to sensor quantization.

We ran simulations with 6S for parameters corresponding to ranges observed in the Landsat data (aerosol optical thickness at 550nm between 0.01 and 0.2, water vapour concentration between 1.5cm and 2.5cm, ozone concentration between 0.32cm and 0.35cm, ρ_{red} between 0.02 and0.28 and ρ_{NIR} between 0.21 and 0.52) with a continental atmosphere and vegetation target and surroundings. SR was chiefly sensitive to aerosol optical depth rather than water vapour or ozone. Using a typical uncertainty of 0.05 for optical depth (Kaufmann and Sedra, 2000) we determined for the SR:

$$\varepsilon_{6s} = 0.0071SR - 0.0074 \quad r^2 = 0.88 \qquad (7)$$

To model sensor quantization errors we note that estimated reflectance ρ is given by:

$$\hat{\rho} = \frac{x_a\ell - x_b}{1 + x_c(x_a\ell - x_b)} \qquad (8)$$

where x_a, x_b and x_c are derived using the 6S and ℓ is at sensor radiance. The second term in the denominator is typically O(10^{-2}) while the numerator is at least O(10^0) so we write:

$$\hat{\rho} \approx x_a\ell - x_b \qquad (9)$$

but ℓ is estimated using:

$$\ell = a_0 + a_1 DN \qquad (10)$$

where DN is sensor count and a_0 and a_1 are offset and gains respectively. Assuming a uniform distribution of quantization errors we have a 1σ error in DN of 0.28DN giving:

$$\varepsilon_\rho \approx \frac{0.28 x_a a_1}{\rho} \qquad (11)$$

Using mean values of x_a over all simulations (the coefficient of variation is less than 10%) and a_1 from GICS reports for the scenes used gives ε_ρ of $1.27\text{x}10^{-3}\rho^{-1}$ for, $1.4*10^{-3}\rho^{-1}$ for NIR. Typical values of ρ for vegetation results in less than 4% for ε_{RED} and ε_{NIR}.

The total 1σ error budget for less than 12% for SR from Landsat TM 5 at a SR of 15 assuming a 4% relative calibration error between red and NIR bands. The error budget for Landsat ETM is lower since $\varepsilon_{NIR/red}$ is given as 1% and in-situ aerosol optical depth measurements was used. However, the additional error in back-calibrating the ETM data to the TM 5 data will tend to counter this reduction.

Comparison of Empirical *L* Estimators

Satellite measurements of SR are, in general, responsive to both overstory and understory ***L***. However, our surface measurements were intended to correspond to overstory ***L***. We have included an error term in the L budget to account for overlap of overstory and understory foliage. But, the impact of unmeasured leaf area on the relationship between SR and measured overstory ***L*** is relegated to noise in the regression.

Figures 1a through c illustrate the trends between observed ***L*** versus ***SR*** stratified by leaf type. The increase in scatter with increasing ***SR*** and ***L*** is due to both physics and measurement errors. Physically, the sensitivity of top of canopy reflectance to ***L*** is inversely proportional to ***L*** (Sellers, 1985). In terms of measurement errors, red reflectances are often on the order of 2-3% for observed simple ratios above 15. Both atmospheric correction error and quantization error is therefore largest at high SR. Regression fit residuals without transformation are heteroscedastic and should not be applied although this has been the case in the majority of previous studies. A log transform was applied to ***SR***. A power transform (exponent 0.25) was applied to ***L*** since a log transform would overly emphasise additive errors due to understory ***L***. A Type II (structural) regression (Kendall and Stuart, 1951) and +/-2σ confidence intervals of ***p(LAI|SR)*** are shown an Figure 1.

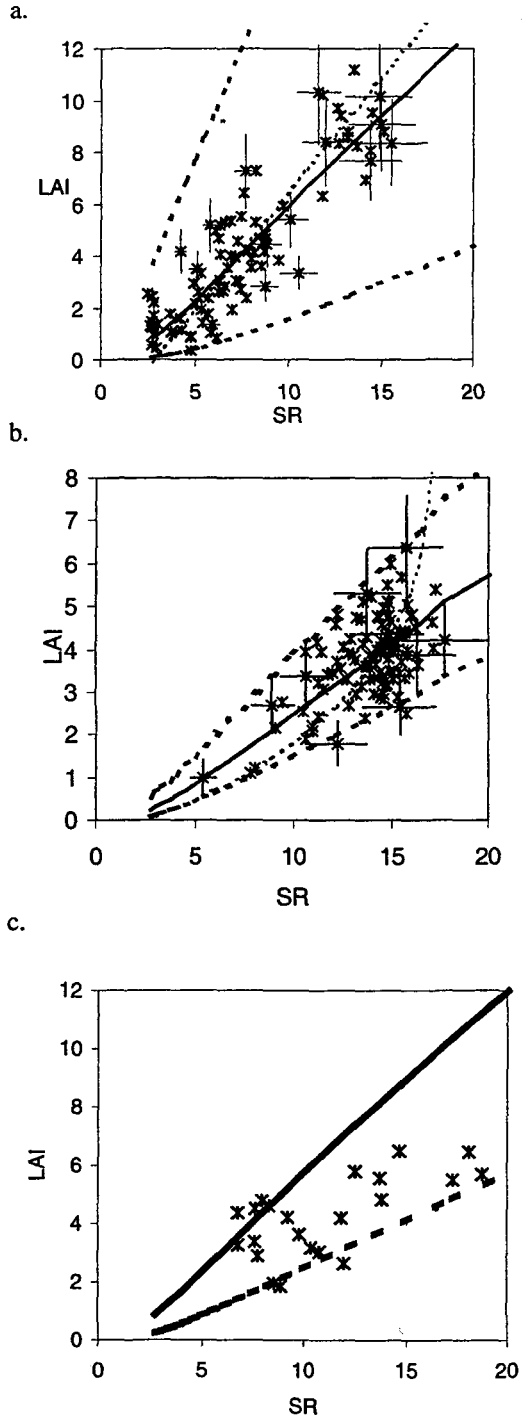

Figure 1. Empirical estimation of ***p(L|SR)*** from a needleleaf b. broadleaf and c. mixed sites surface measurements and Landsat TM based ***SR*** across Canada. Modelled measurement error bars are shown for a sub-sample of needleleaf and broadleaf stands

Solid lines in 1a and 1b are Type II m.l.e. curves while dashed are corresponding +/-2σ intervals. Dotted lines in 1a and 1b are Type I m.l.e. curves.

The influence of measurement error of remotely sensed quantities on regression has been considered previously using the reduced major axis method (Curran and Hay, 1986) when applied to canopy cover estimation (Larsson, 1993) However, the RMA estimate does not produce the maximum likelihood unbiased regression estimate as derived in Kendall and Stuart. Our use of Type II regressions is in contrast to other empirical L studies that assume either error free L or SR measurements (e.g. Ripple, 1985; Peterson et a. 1987; Spanner et. al. 1990; Chen and Cihlar, 1996; Brown et al. 2000; Chen et al. 2001). For comparison we include Type I regressions using the assumptions adopted in Chen et al. (2001).

Additionally, we suggest that it is sufficient (and preferable) to show the confidence intervals of $p(L|SR)$ rather than either the coefficient of determination or standard error since these latter parameters are only marginal aspects of the quantity of interest (i.e. $p(L|SR)$). The confidence intervals get wider with increasing L both due to the increase in scatter and, for needleleaf stands, due to a bias in sampling to lower L stands.

Physically Based Estimation of L

Models exist that relate physical properties of canopy, soil, sensor and sky irradiance to the integrated intensity and net flux of energy within and at the boundary of the canopy (Myneni and Ross, 1991). It is possible to define a family of models that conserve quantities of energy, mass and momentum at the expense of a large number of parameters to specify the entire range of canopy realisations we expect over large areas. Given both the additional uncertainty in parameters with more complex (physically realistic) models and our desire to focus on nadir SR versus L relationships we decided to use simplified models that have been validated with field measurements over a number of sites.

We adopted a well studied two-stream plane-parallel radiative transfer model that has been proven to explain variability in nadir broadband reflectance relatively well for homogenous broadleaf canopies (Sellers, 1985). We did so at the expense of ignoring controls on reflectance due to foliage clumping. Clumping has been demonstrated to be important in characterising nadir reflectance of conifer stands through the use of geometric-optics models such as 4-Scale (Chen and Leblanc, 1997). We selected a simplified version of 5-scale, FLAIR (White et al. 2001), in an effort to capture controls of L and clumping on reflectance while reducing demands in both specification of other model parameters (e.g. crown dimensions) and numerical computation. FLAIR was modified to include an estimate of multiple scattering using the Sellers model with a simple reduction in L based on the clumping factor.

Both models were run over a wide range of parameter values measured over vegetated surfaces in Canada and northern United States. All runs assumed clear sky conditions with 35° solar zenith angle representative of the TM data used. Each run provided a realisation, c_i, of (L,SR) given an input parameter vector x.We estimated $p(L,SR|p(x))$ by varying x over some joint pdf $p(x)$. As in Knyazhkin et al (1998) we ran the physically based model with $p(x)$ equal to the unifrom joint distribution of x (i.e. $u(x)$).

Semi-Empirical Approach

In general $p(x)$ is not uniform. For example, mineral soils and needle litter often exhibit a linear relationship between nadir reflectance and wavelength. Furthermore, simplifications in the reflectance models will result in both large area and local errors in $p(L|SR,p(x))$. Assuming C is an unbiased sample across x we used $p(x)=p(x|C)$ rather than u. Then,

$$p(x \mid C) = \max_i p(x \mid c_i) \qquad (12)$$

where $p(x|\, c_i)$ is specified by the error models for SR and L and c_i are mutually independent. Figures 2 and 3 show $p(L|SR,u(x))$, where u is the uniform distribution, for selected values of SR together with empirical and semi-empirical estimates.

Results

Empirical Model

The majority of the broadleaf measurements were for mature forests and productive crops so low L values are undersampled. Measurements during leaf out or senescence are not included due to the need to recalibrate α. Needleleaf data covered a fairly large range of L and SR values and exhibit nearly constant scatter of SR across L. Low L conifer stands are typically heterogeneous in spatial foliage distribution and understory characteristics. The scatter in the

national data set is then a limitation of pooling data across a number of species, growing condition, soil types and understory cover. There was insufficient mixed forest data to support a regression model. In addition, a separation of needleleaf and broadleaf contribution to L was not available. Rather, the mixed forest data was used to evaluate our current approach to estimation of LAI over mixed sites.

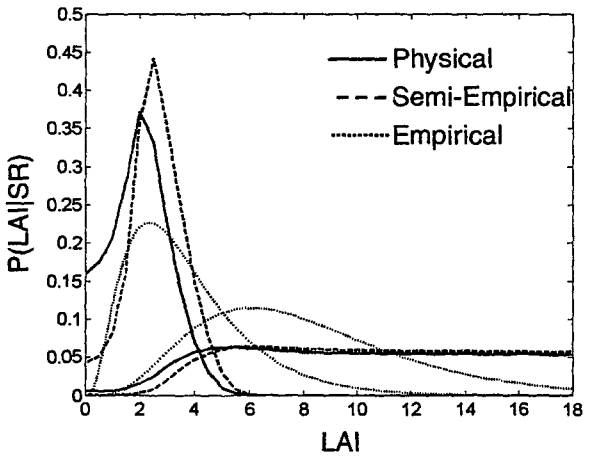

Figure 2. Comparison of physical, semi-empirical, and empirical estimates of $p(L|SR,x)$ for conifer stands at at SR of 5 (curves on left) and 10 (curves on right). Physical estimates are shown for both $p(x)=u(x)$ and $p(x)=p(x|C)$.

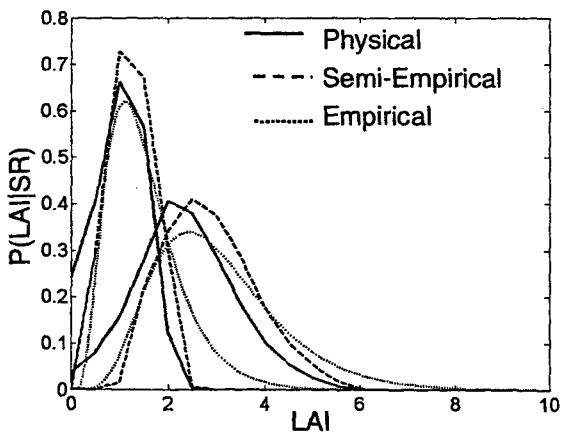

Figure 3. Comparison of physical, semi-empirical and empirical estimates of $p(L|SR,x)$ for broadleaf stands at SR of 5 (curves on left) and 10 (curves on right).

Type II regressions were almost linear for both needleleaf and broadleaf sites although it must be remembered that the regressions are from non-linear transformations of the fitted lines. The $+/-2\sigma$ intervals encompassed most of the data suggesting that outliers did not unduly influence the regressions. The needleleaf interval was substantially larger than that for broadleaf. The interval was fit in transformed space so it tended to increase as L and SR increases in linear space. This is a purely empirical result although we shall see that it was also reflected in the physical models. The intervals likely overestimate local uncertainties in L as well as the potential precision of locally calibrated algorithms since they reflect scatter due to variability in conditions across Canada. However, we believe the increasing confidence interval width as L increases is a better reflection of known errors in L and SR than an interval derived from a regression applied in untransformed (linear) space. This is further supported for the deciduous data where the sampling distribution of L was fairly uniform over middle and high L ranges. Additional samples for high L needleleaf stands would likely reduce the current large uncertainty in $p(L|SR)$ for this data set.

There is potential for bias when using Type I regressions with broadleaf sites (Figure 1b). In contrast, the bias error was smaller for needleleaf stands due to the more even distribution of samples across L and the increased scatter at low L. However, even with needleleaf stands, fitting regression models in untransformed space results in smaller confidence intervals (not shown for brevity) than those predicted by Type II or physical methods.

Figure 1c indicates that the empirical fits tend to support a smooth transition between broadleaf and needleleaf models. Furthermore, the available mixed forest data lies close to or within the envelope formed by the curves. In summary we suggest the following empirical models for estimating the maximum likelihood estimate (m.l.e.) of L given SR across Canada in the absence of additional information:

$$L=\begin{cases}(0.449\ln SR+0.514)^4 & \textit{needleleeaf}\\ (0.424\ln SR+0.276)^4 & \textit{broadleaf}\end{cases} \quad (13)$$

and a linear weighting of these two models for mixed stands by fraction of needleleaf and broadleaf cover. It should be remembered that this refers to overstory L only.

Equation 13 only provides m.l.e. under the constraints of measured data. Encouragingly, the m.l.e. from the physically based model generally agrees with that of the empirical model. Figures 2 and 3 indicated that substantial differences in $p(L|SR)$ occur at $L<1$ and $L>5$. At low L both the lack of surface measurements and uncertainties in co-locating surface measurement footprints with satellite measurements suggest the physically based model is

preferred. Furthermore, we currently used a two-parameter linear fit (in transformed space) for the empirical regression.

A comparison of the physical model and empirical estimates, shown in Figures 4 and 5, suggest that the actual relationship between ***SR*** and ***L*** may be more complex (if we believe the physical model) and may not be similar for high and low ranges of ***L***. The physical model also results in a much larger range of ***p(L|SR)*** at low ***SR*** due to the use of ***u(x)***. Essentially, low ***SR*** simulations correspond to cases where understory variability has a larger effect on overstory ***SR*** and therefore ***p(L|SR)*** is more sensitive to the joint distribution of overstory and understory model parameters. Figures 2 and 3 indicate that at higher values of ***L*** the physical model reaches a saturation point (*sensu* Knyazihkin et al., 1998) where ***p(L|SR)*** is nearly uniform over a large range. Evidently an m.l.e. estimate using the physical model alone is ill-conditioned as a mode does not seem to exist. However, one must remember that there are other constraints of ***p(L)*** from the environment. For example, if we assume that our measured dataset ***C*** captures these other constraints then we have a relatively well defined estimate of ***L*** even for higher SR. Evidently, the resolution of ***p(L|SR)*** is insufficient for unbiased estimates of L at higher values of ***L***. Other remote sensing methods such as multi-angle retrieval (Knyazihkin et al., 1998), LIDAR (Lefsky et al. 1999) measurements may provide more precise estimates of ***p(L)***. In any event, confidence intervals of physical models and empirical models should be compared rather than simply accepting the m.l.e. estimate of the physical model.

While our national data set is not sufficient to also estimate an a priori ***p(L)*** we do use it to constraint p(x). Figures 2 and 3 show there is closer agreement between empirical and physical models after constraining simulations using ***p(x|C)***. Furthermore, as indicated in Figures 4 and 5, the physical model tends to support the increase in the confidence intervals of ***p(L|SR)*** with increasing ***L***; both in magnitude and skew. Comparison of the coverage of the semi-empirical and empirical model also allows us to identify areas where the empirical data set is sufficient (e.g. ***L*** ranging from 3 to 5 for deciduous and from 1 to 6 for conifer) and is lacking.

Based on our results we conclude that:

1. Estimation errors were below 20% for ***L*** assuming no understory contribution to measurements and 12% for ***SR*** .
2. Type II regressions on transformed data were appropriate for estimating ***L*** using empirical methods. This is in contrast to other studies that have applied Type I regressions in untransformed space to similar empirical data sets.
3. Conditional on our limited sample two parameter regressions for m.l.e. estimates of ***p(L|SR)*** for needleleaf and broadleaf were provided. Equal weighting is suggested for mixed stands in the absence of cover fraction data. Empirical m.l.e. estimates should be used for ***L***>5 while physically based estimates are preferred for ***L*** <1. Our method of constraining the input parameter space for the physical method using measurements allows for more appropriate estimates of ***p(L|SR)***.

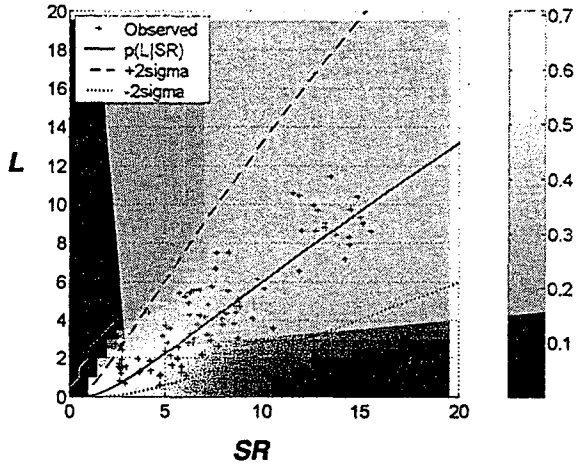

Figure 4. Density plot of ***p(L|SR)*** for needleleaf stands using the semi-empirical method and Type II regression and confidence intervals and observations.

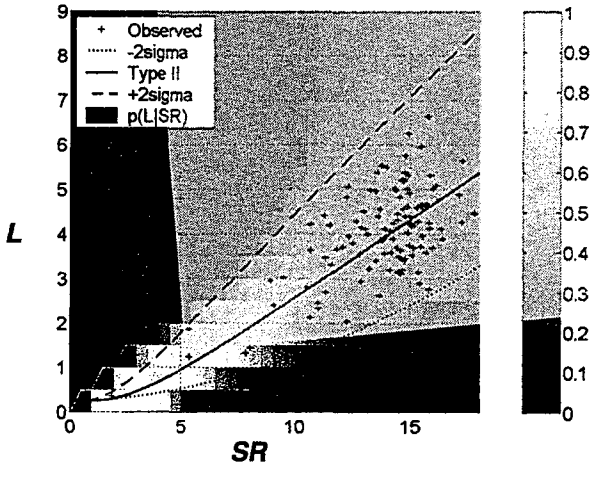

Figure 5. Density plot of $p(L|SR)$ for broadleaf stands using the semi-empirical method and Type II regression and confidence intervals and observations

Our study was limited to relatively healthy green-foliage under natural conditions except for the agricultural sites. Furthermore, all of the sites were near peak growing season conditions without apparent stress. In addition, we did not consider sites with substantial thatch, extreme planophile or erectophile leaf angle distributions or well separated overstory strata as in shelter-wood plantations. These issues will need further research, both in surface measurement and remote sensing.

Appendix A

To prove Equation (5) we have from Miller (1963):

$$L = 2\int_0^{\pi/2} f(\theta)\sin\theta d\theta \qquad \text{(A1)}$$

Where $f(\theta)$ is the average number of contacts per unit length traversed in the canopy along θ when Ω=1. Assuming Equation 1 is valid, the number of contacts when Ω is not equal to one is given by:

$$f_\Omega(\theta) = -\frac{\ln P(\theta)\cos\theta}{\Omega(\theta)} \qquad \text{(A2)}$$

But, Equation 1 and EquationA2 gives:

$$f_\Omega(\theta) = \Omega(\theta) f(\theta) \qquad \text{(A3)}$$

Substituting Equation A2 into A1 gives Equation 5:

$$L = 2\int_0^{\pi/2} -\frac{\ln P(\theta)}{\Omega(\theta)}\cos\theta\sin\theta d\theta \qquad \text{(A4)}$$

Acknowledgements

Field data was provided by J.A. Trofymow, D.R. Peddle, J. Van der Sanden, E. Swift. D. King, I. Oltoff, E. Seed and L. Brown. This analysis and reporting of results was supported by NRCan (Environmental Monitoring Section of CCRS).

References

Brown, L., J.Chen, S. Leblanc and J. Cihlar. 2000. A shortwave infrared modification to the simple ratio for LAI retrieval in Boreal forests: An image and model analysis. *Remote Sens. Environ.*, 71:16-25.

Chen, J.M. and J. Cihlar, 1995. Plant canopy gap-size analysis theory for improving optical measurements of leaf-area index. *Applied Optics*, v. 34: 6211-6222.

Chen J., 1996. Optically-Based Methods for Measuring Seasonal Variation of Leaf Area Index in Boreal Conifer Stands. *Agricultural and Forest Meteorology*, 80:135-163.

Chen J. and J. Cihlar. 1996. Retrieving Leaf Area Index in Boreal Forests Using Landsat TM Images, *Remote Sensing of Environment*, 55 :153-162.

Chen J. M. and S.G. Leblanc, 1997. A Four-Scale Bidirectional Reflectance Model Based on Canopy Architecture. *IEEE Trans. Geosci. Rem. Sens.*, 351316-1337.

Chen, J., P.W. Rich, S.T. Gower, J.M. Norman, and S. Plummer, 1997. Leaf area index of boreal forests: Theory, techniques and measurements. *J. Geophys. Res.*, 102(D24): 29029-29042.

J. M. Chen, G. Pavlic , L. Brown, J. Cihlar, S.G. Leblanc, P. White, R. J. Hall, D. Peddle, D.J. King, J. A. Trofymow, E. Swift, J. Van der Sanden and P. Pellikka. 2001. Validation of Canada-wide leaf area index maps using ground measurements and high and moderate resolution satellite imagery, submitted to *Remote Sensing of Environment.*

Curran, P. and A.M. Hay. 1986. The importance of measurement error for certain procedures in remote sensing at optical wavelengths. *Photogrammetric Engineering and Remote Sensing*, 52:229-241.

Fernandes, R.A., J.R. Miller, J. Chen and I. Rubinstein, 2000. Evaluating image based estimates of leaf area index in Boreal conifer Stands over a range of scales using high-resolution CASI imagery, Accepted. Remote Sensing of Environment.

Gower, S.T., J. Vogel, T. Stow, J. Norman, S. Steele, and C. Kucharik, 1997. Carbon distribution and aboveground net primary production in aspen, jack pine and black spruce stands in Saskatchewan and Manitoba, Canada, *J. Geophys. Res.*, 102(D24): 29029-29042.

Gower, S.T., C.J. Kucharik, and J.M. Norman. 1999. Direct and indirect estimation of leaf area index, fAPAR and net primary production of terrestrial ecosystems. *Remote Sensing of Environment*, 70:29-51.

Kaufmann, Y. and Sendra. 1988. Algorithms for atmospheric correction. *Int. J. Rem. Sens.* 9:1357-1381.

Kendall, M., & A. Stuart, 1951. The advanced theory of statistics (Vol. 2). New York: Hafner.

Knyazikhin, Y., 1998. Synergistic algorithm for estimating vegetation canopy leaf area index and fraction of absorbed photosynthetically active radiation from MODIS and MISR data. *J. Geophys. Res.*, 103:32,257-32,276.

Kucharik, C. J., J. M. Norman, L. M. Murdock, and S.T. Gower. 1997. Characterizing Canopy Nonrandomness with a Multiband Vegetation Imager (MVI) *J. Geophys. Res.* 102: 29,455-29,473.

Larsson, H. 1993. Linear regression for canopy cover estimation in Acacia woodlands using Landsat-TM, -MSS and SPOT HRV XS data. *Int. J. Rem. Sens.*, 14:2129-2136.

Leblanc, S. and J. Chen, 2001. A practical scheme for correcting multiple scattering effects on optical LAI measurements, submitted to *Agriculture and Forest Meteorology*.

Lefsky, M.A., W.B. Cohen, S.A. Acker, T.A. Spies, G.G. Parker and D. Harding. 1999. Lidar remote sensing of biophysical properties and canopy structure of forest of Douglas-fir and western hemlock. Remote Sensing of Environment 70:339-361.

Levy, E.B. and E.A. Madden, 1933. The point method of pasture analysis. *New Zealand Journal of Agriculture*, 46, 267-270.

Miller, J.B. A formula for average folage density. *Aust. J. of Bot.*, 15:141-144.

Myneni, R.B. and J. Ross, editors, 1991, Photon vegetation Interactions: applications in optical remote sensing and plant ecology. New York: Springer Verlag.

Nemani, R., L. Pierce, S. Running and L. Band. 1993. Forest ecosystem processes at the watershed scale: sensitivity to remotely-sensed leaf area index. *Int. J. Rem. Sens.* 14:2519-2534.

Nilson, T. 1971. A theoretical analysis of the frequency of gaps in plant stands. Agric. Meteorol., 8:25-38.

Olthof, I., D.J. King and R.A. Lautenschlager, 2001. Leaf area index changein ice storm damaged sugar maple stands. *Forestry Chronicle*. Accepted.

Peterson, D.L., M.A. Spanner, S.W. Running and K.B. Teuber, 1987, Relationship of Thematic Mapper simulator data to leaf area index of temperate coniferous forests. *Remote Sens. Environ.* 22:323:341.

Ripple, W.J. 1985. LANDSAT Thematic Mapper bands for characterizing fescue grass vegetation. *Int. J. Rem. Sens.*, 6:1373-1384.

Sellers, P.J., 1985. Canopy reflectance, photosynthesis and transpiration. *Int. J. Remote Sens.*, 6:1335-1372.

Teillet, P.M., J.L. Barker, B.L. Markham, R.R. Irish, R.R., G. Fedosejevs, G. And J.C. Storey, Radiometric Cross-Calibration of the Landsat-7 ETM+ and Landsat-5 TM Sensors Based on Tandem Data Sets, *Remote Sensing of Environment*, in press.

Vermote, E.F., D. Tanre, J.L. Deuzé, M. Herman, and J.J. Morcrette, 1997. Second simulation of the satellite signal in the solar spectrum, 6S: An overview., *IEEE Trans. Geosc. Remote Sens.*, 35(3):675-686.

Warren-Wilson, J., 1958. Inclined point quadrats, *New Phytologist*, 51:1-8.

White, H.P., J.R. Miiller, and J.M. Chen, 2001, Four-Scale Linear Model for Anisotropic Reflectance (FLAIR) for Plant Canopies. I: Model Description and Partial Validation, IEEE *Trans. Geosc. Remote Sens.*, in press.

Whittaker, R.H. and G.M. Woodwell, 1967, Surface area relations of woody plants and forest communities, *American Journal of Botany*. 54:805-929.